IN-ORBIT SPACE-BASED SURVEILLANCE SYSTEM BY HIGH-PERFORMANCE COMPUTER-VISION ALGORITHMS AND DEDICATED HW AVIONICS

D. Gonzalez-Arjona[1], M.A. Verdugo[1], V. Pesce[1], A. Alcalde[1], D. Gogu[2], V. Ghisoiu[2], S. Erb[3], P Tesani[3]

[1])*GMV Aerospace and Defence SAU, C/ Isaac Newton, no. 11, PTM 28760, Madrid, Spain, Email: {dgarjona, maverdugo, vpesce, aalcalde}@gmv.com*
[2] *GMV Innovating Solutions SRL, SkyTower, 32nd floor, 246C Calea Floreasca, 014476, Bucharest, Romania,, Email:{dgogu, vghisoiu}@gmv.com*
[3] *European Space Agency – ESTEC, The Netherlands:{sven.erb, paride.tesani}@esa.int*

ABSTRACT

GMV is developing an experimental payload focused on the assessment of in-orbit satellite servicing for tracking debris in MEO/LEO making use of ad-hoc solutions for high-performance computer-vision algorithms, FPGA implementation and new dedicated equipment development for a stand-alone smart-sensor HW combining optics, imaging sensor and computing electronics in a reduced shaped unique enclosure. The SBSS-GNSS (Space-Based Surveillance System) would be hosted as experimental payload on board Galileo satellites of Galileo constellation for offering debris surveillance with main focus in Galileo orbits (MEO) as secondary service for monitoring and detection the proliferations of debris in the most populated space area.

Keywords: Debris detection, on-board processing, Galileo, FPGA, Smart-sensor, camera, space, microelectronics, equipment

1. INTRODUCTION

In the frame of Space Situational Awareness (SSA), space-based assets can be used to complement and enhance the capabilities of a ground-based network of sensors (mainly surveillance and tracking radars and optical telescopes) for the support of the Space Surveillance and Tracking (SST) and Near-Earth Objects (NEO) segments. GMV is interested in proving key technologies on-board of the next generation Galileo Satellite as a market position opportunity to extend their existing ground-based products to this respect. Hosting the SBSS-GNSS payload on a Galileo satellite would seem a cost-effective approach besides the technical and operational benefits that will provide. Observation of objects in MEO and LEO can be covered by ground-based radar or optical telescopes, the case for a space-based surveillance system is considered as particularly interesting for observation of objects from a different perspective complementing the observations obtained from ground while presenting certain advantages such as higher performances due to

absence of atmosphere and good timeliness. Space-based techniques significantly improves the results achievable with ground-based techniques by reducing the observable debris size and by enabling observations for different orbits.

The proposed experimental payload consists on a miniaturized independent system which is able to detect debris, through dedicated image processing algorithms accelerated on-board by a HW implementation. The computer-vision solution process images performing various filters looking for debris candidates in the FOV of the camera. The algorithms includes the detection and tracking of potential debris objects, being the detected candidate features in the images. The candidates screening and selection includes different considerations such as the detection of light curves, the different relative motion of stars vs potential debris and the geometrical expected motion and detection over consecutive frames. A preliminary assessment has been already performed evaluating four different cases of debris orbits (taken from results of the PROOF SW tool analysis) keeping fixed the size of the debris. The orbital characteristics are quite different leading to different velocity of the debris on the camera sensor. Distinct values of this quantity, here called "Dwell Rate", are analyzed from 1.4 pxl/s up to 7.5 pxl/s.

2. CONCEPT ANALYSIS

The first step in the design process is to perform a concept analysis to verify the capabilities of the payload and to identify its limitations. One of the key elements of the proposed architecture is the implementation of dedicated algorithms for detection and tracking of dynamics objects (debris). The debris may be very dim in the image and, in general, its brightness strongly depends upon distance (and other parameters). A way to quantify its brightness is through the signal-over-noise ratio (SNR). This value is function of numerous other parameters:

- Apparent Magnitude of the debris (function of relative distance, debris absolute magnitude and Sun phase angle)

- Camera Physical Parameters.
- Integration Time.

Being so many different quantities involved in the definition of the SNR, an analysis is necessary to highlight different conditions in many possible scenarios to better define the operational requirements.

2.1. Apparent Magnitude Analysis

The first analysis that is carried out concerns the apparent magnitude of the debris. This is an essential figure to be quantified to assess the overall achievable SNR. In particular, the apparent magnitude depends on the relative distance between the debris and the camera mounted on the Galileo spacecraft, on the debris size and albedo and on the Sun phase angle. Knowing these quantities, the apparent magnitude of an object can be computed, as commonly done, approximating the debris as a Lambertian (diffusely-reflecting) sphere. The change of apparent magnitude function of debris size and relative distance, fixing the Sun phase angle, are reported in Table 1.

ρ \ d	5mm	1cm	10cm	30cm	50cm	70cm	1m	1.5m	2m
100m	-1.48	-2.98	-7.98	-10.37	-11.48	-12.21	-12.98	-13.87	-14.49
1km	3.52	2.02	-2.98	-5.37	-6.48	-7.21	-7.98	-8.87	-9.49
100km	13.52	12.02	7.02	4.63	3.52	2.79	2.02	1.13	0.51
1000km	18.52	17.02	12.02	9.63	8.52	7.79	7.02	6.13	5.51
4000km	21.53	20.03	15.03	12.64	11.53	10.80	10.03	9.15	8.52
10000km	23.52	22.02	17.02	14.63	13.52	12.79	12.02	11.14	10.51
20000km	25.03	23.52	18.52	16.13	15.03	14.29	13.52	12.64	12.02

Table 1. Apparent Magnitude - Sun Phase Angle = 20º

As expected, fixing the size of the Sun phase angle, the size of the debris strongly influences its apparent magnitude. Moreover, closer objects have lower magnitude, therefore, they appear to be brighter. This analysis also gives an idea of the apparent magnitude of a debris at different distances.

2.2. SNR Analysis

The second and most important analysis involves the direct calculation of the SNR depending on physical and orbital parameters. The SNR is computed using an augmented list of sources considered as contributors to the noise budget as in [1]. To carry out this analysis, the noise parameters of the detector CMV4000 and optics Tele-Xanar 2.2/70 are considered. The results in Figure 2.2-1 show the reachable SNR considering an apparent magnitude of the target and a given exposure time. As expected, an increase in the exposure time is directly translated in a higher achievable SNR given the same debris apparent magnitude. The constraint for a correct debris detection derived from the IP of SNR=5 for a debris of magnitude 13 is satisfied only for exposure times longer than 1s.
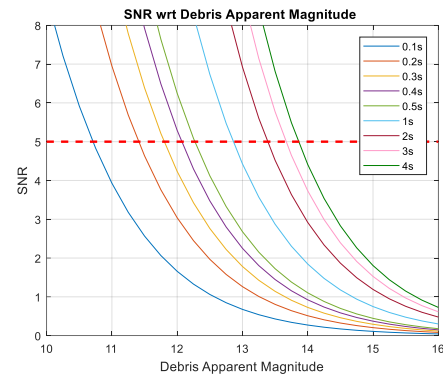

Figure 2.2-1.SNR wrt apparent magnitude for different t

2.3. Observability Analysis

In order to evaluate the detection probability of debris depending on the camera characteristics and orientation, the ESA PROOF (Program for Radar and Optical Observation Forecasting) software is used **Error! Reference source not found.**. This tool provides statistical pass characteristics of the non-deterministic space debris population and as well as the acquisition and pass characteristics of known objects for ground- and space-based radar and passive optical sensors. For the camera parameters, the values in Table 2 are adopted.

Parameter	Value
Aperture Diameter	0.075 [m]
Field of View	4.27 [deg]
Number of pixel per row	1024 (considering a 2x2pxl binning)
Integration time	1 [s]
Min. number of consecutive detections required	3

Table 2 PROOF Simulation Parameters

A single run statistical simulation of the duration of one orbit is executed, considering a debris lower threshold diameter of 0.01m and an upper one of 2m. Representative Galileo orbit and attitude profile is simulated. Different materials and related albedo values are used by the PROOF software to generate the debris population. To help visualize the obtained results, orbits and the crossing/detected debris are reproduced in Figure 2.3-1, for a single case. In the plot, the crossing debris are depicted in black, the detected ones in red and their orbits in dotted red, moreover, the LOS of the camera is plotted as a green arrow every 5º.
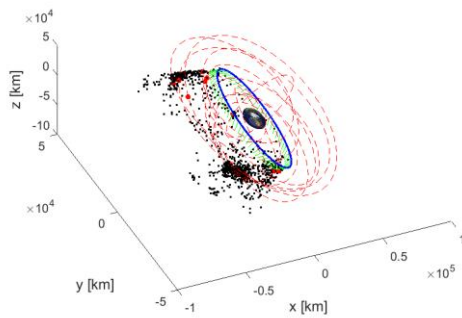
Figure 2.3-1. 3D orbits of detected debris

As results of the concept analysis, some general considerations can be made:

- The LEO region can't be observed because of geometrical reasons involving Earth exclusion angle. In fact, to avoid straylight effects, an appropriate baffle should be adopted resulting in an unfeasible mechanical solution. Moreover, the detectable debris dimension at MEO altitude would be very high (in the order of more than 2m) and, therefore, it would not represent a significant contribution to the actual ground based surveillance systems for LEO.
- The minimum size of the detected debris is in the order of few tens of centimetres.
- Exposure times in the order of 1-2 seconds are recommended to maximize the detectable objects.
- Focal length greater or equal than 100mm (or better, aperture diameter greater than 50mm) are recommended to maximize the detection probability.

3. IMAGE PROCESSING

A dedicated image processing algorithm, derived from previous projects at GMV for long-range image processing, was revised and adapted for this project. The baseline algorithm is described below

- *Stage 0*: Image acquisition and radiometric correction as in Figure 3-1.
- *Stage 1*: Image binarisation.
- *Stage 2*: Candidate screening: A check is devised that eventually isolates the candidates corresponding to target(s) from the much larger set of spurious candidates in the binarised frame. The filter exploits that the targets usually move slowly across the detector whereas the stars cross quickly the field of view, i.e., a target appears in nearby positions in successive frames. Stars may pass near a target and seed new spurious candidates. No corrective action is necessary but the track is temporarily lost.

- *Stage 3*: Screened frame analysis. The screened frame is analysed to assess whether it contains only pixels of the target or targets.
- *Stage 4*: Centroiding of the target object(s). The centre of brightness is calculated for the target objects that have been identified and validated in the prior stage.

Figure 3-1. Calibrated image

4. AVIONICS SYSTEM ARCHITECTURE

Dedicated development of new avionics technologies is driven by the needs of all areas of space applications for image processing and camera optical unit developed and joined in the same enclosure. The dedicated avionics include two rad-hard FPGA, European NG-MEDIUM and high-performance Virtex5QV. A smart sensor concept is proposed including processing electronics and the needed space acquisition camera embedded within the miniaturized electronics and directly connected to NG-MEDIUM, in charge of both the image acquisition and also external/internal interfacing. The concept is an evolution of Image Processing Board as previously being developed in different GMV activities [1] but including in this case also the camera logic, detector, optics and baffle in the same HW. While embedding a camera, the system also allows the connection of eventual second external camera that can supply images from different satellite locations and pointing, covering bigger or complementary areas. Through direct connection with embedded imaging sensor it is managed the configuration, commanding and acquisition of images using FPGA logic and applying pre-processing in streaming pipeline. Avionics incorporates a second FPGA dedicated to the implementation and HW-acceleration of the computer-vision algorithms, the most computationally demanded part. The FPGA high performance solution allow more consecutive frames being processed thanks to the utilization of FPGA and the pipeline processing in streaming thanks in part to the integration of the logic for the camera images acquisition in the presented embedded HW solution.

The key HW modules can be summarized as follows:

- Main Stage Power Input module,
- Second Stage Power module,
- Interface Communication Control & Image Acquisition module,
- Image Sensor module,
- Data Processing Control module.

The impact of a significant miniaturization of avionics system has been studied in the framework of a complete solution for Camera and image processing system joined together studied for the second generation of Galileo satellites constellation.

The effect of combining the traditional avionics elements by a complete system has been analyzed, and the impact on avionics mass, power, volume, operability, complexity, risk and cost for the avionics architecture has been studied.
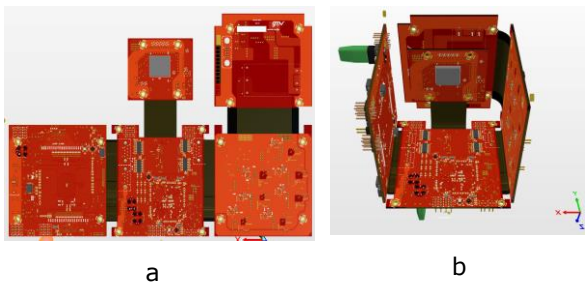

a   b

Figure 4-1. Avionics unfold state (a), fold state (b)

The avionics module board architecture is composed of two different interconnected main areas:
- Data Interface Communication Control & Image Acquisitions, which the NG-Medium FPGA as the main processor. This area is connected to the interface of the system and to the the Image Sensor module.
- Data Processing Control, withs the Virtex-5 FPGA as the co-processor. This area is used for high-performace image processing.

For storing the captured images and various maintenance services, the NG-Medium FPGA uses a SDR SDRAM memory.

For supporting the processing alhorithms, DDR2 memory is selected. The part will allow fast transfer by using dual data rate and burst funcionalities.

Data exchange between the Data Interface Communication Control & Image Sensor module and the Data processing module is enabled by parallel interface using a full duplex 8 bit transmission solution. The solution require at least 23 connection for the link between the two FPGAs.

The avionics is interfacing using nominal and redundant SpW links with the OBC and it can interface and control second camera via SpW Link.

5. IP HARDWARE IMPLEMENTATION

The IP implementation consists of three main parts (image pre-processing, segmentation of bodies with candidate screening and tracking) with different stages described below:
- *Stage 0*: Image binarization and storage in a buffer of past images. A defined number of images are integrated into a single image.
- *Stage 1*: Dilation. Some star trails can become discontinuous depending on binary threshold value. This stage is meant to merge and form a continuous trail. It also simplifies cases with star clusters reducing the number of blobs.
- *Stage 2*: Closing. Dilation and then an erosion. Used to fill regions inside star trails or star clusters.
- *Stage 3*: Segmentation. Contours of every blob are found. Each group of pixels that are close together are considered as the same blob. These minimal bodies are used as base for applying next steps.
- *Stage 4*: Blob feature extraction. The angle of every blob with respect to the horizontal is calculated. The principal diagonal is used for calculating the angle. The values are represented as an angle histogram. The most frequent value corresponds to the star trails direction since the stars, that represent the majority of blobs, move apparently in the same direction and the debris will likely follow a different direction.
- *Stage 5*: Candidate screening. Possible candidates for debris are those blobs whose angle is not inside the interval centered at the star trails angle and a defined threshold. This threshold accounts for the errors due to discretization (resolution is limited by discrete pixel size and star trail thickness). This value depends on the technical specifications of the camera and sensor.
- *Stage 6*: Tracking. After the candidates are detected, they are stored in a buffer of past screened candidates. All these candidates are added together, in order to integrate the candidates over time. This gives a new image in which the direction of each one can be calculated using a modified version of the previous stages without the need of calculating the histogram of star trails. The angle used is the same calculated previously in original entire image. Remaining candidates are count as detected debris.

6. MECHANICAL HW DESIGN & MOUNTING

The enclosure structure is designed to accommodate all the electronics and the system optics. The walls thickness and top cover of the enclosure have 4 mm, 4 x 4M mounting holes are dedicated for the top part of the enclosure, 8 x 3M mounting holes for the internal support of the electronics, 4 x 4M for the Baffle and 8 x 4M screws are used for to fix the enclosure onto the tilting platform. The camera tilting platform it is

composed by 2 different parts, the static one that will be mount on the satellite by means of 9 x 4M screws and the adjustable platform where the camera will be fixed, giving the advantage of tilting the platform between 0 to 30 degrees. The tilting platform will be also used for thermal dissipation. The platform will be fixed by using 4 x 7.5M screws.
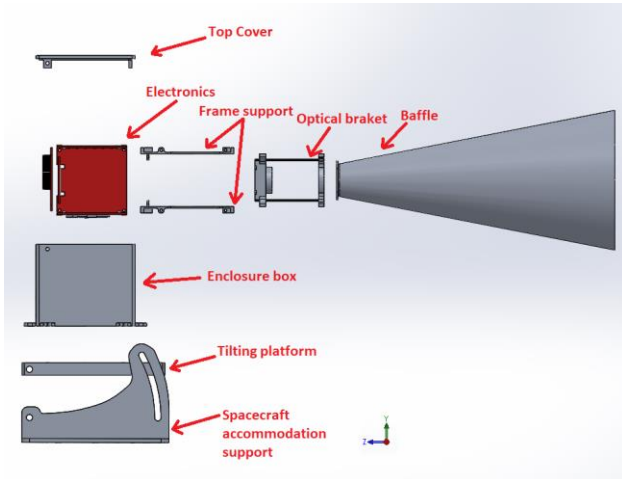

Figure 6-1. Avionics Enclosure

An important structural design feature derived from the accessibility requirement is the presence of the inside frames and optical accommodation structure. The design concept behind this type of structure has been proven in previous mission based on the star-tracker, cameras and cameras on CubeSat.
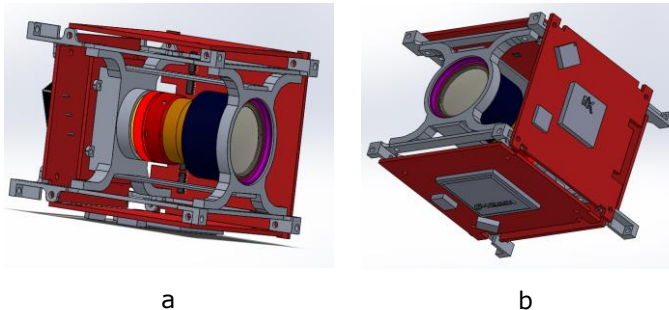

a   b

Figure 6-2. Avionics and lenses fixation (a), (b)

7. FPGA DEVELOPMENT

7.1. Data Interface Communication Control & Image Acquisition FPGA (CIF) based on NGMEDIUM

CIF is responsible for managing, routing and accessing data from/to exterior through different interfaces. CIF is designed as a central manager that controls every other interfaces controller. The modules designed are: Central Manager, Camera Sensor Controller, SpaceWire Controller, Memory Controller, Inter FPGA link (connection with the 2nd FPGA).

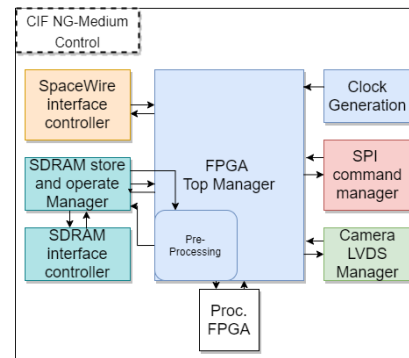The firmware functional architecture and data flow of the CIF is presented below:

Figure 7.1-1. CIF VHDL firmware Design

A central FPGA block Top Manager is responsible of the full SBSS unit interfacing acting as a master router for setting the mastership of all external interfaces driven by commands received on SpaceWire and routing the data inside the CIF, to the Processing FPGA (IPF) or back to the SpaceWire I/Fs. But this unit is not only an interfaces controller as it also includes the camera acquisition functionality and the Pre-Processing part that contains the algorithms that are used in order to correct the raw image received by CIF using Low-Level Image Correction Process algorithms like Bias-Gain correction and Bad-Pixel correction.

The selected external interface is based on SpaceWire that provides a low power and high speed (up to 200Mbits/s in Single Data Rate mode) full-duplex data link. These I/Fs are used to transfer data at high speed: commands from OBC, pre-processing data tables, pixels from a 2nd Camera Optical Unit board and pixels requested by a central host OBC/SMU.

Camera Controller is responsible for decoding the image taken by the sensor and recreate it as a digital data. The data pixels are saved in attached SDRAM. SPI manager is used to configure the Camera Sensor parameters. The physical dynamic memory manager will be divided into different sections in order to store the received image from sensor and the Low-Level Image Correction parameters and access them as requested by the Master Router.

7.2. Image Processing FPGA (IPF) Design (Virtex-5)

The Processing FPGA is the area of the system, mainly devoted to the execution of the Vision-based Debris Detection and Tracking algorithm (VDDT-IP). It operates in parallel with CIF, the other FPGA in the system with which is directly connected through Inter-FPGA Link. IPB-IPF acts as slave in this parallel communication. The internal modules of IPF are represented in the functional architecture presented below.
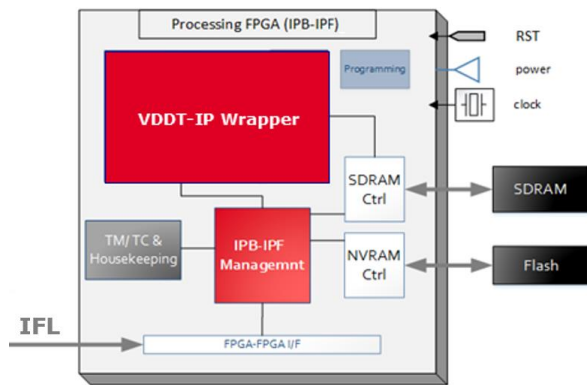
Figure 2: IPF Internal Architecture

The main processing elements is the VDDT IP-core where the Computer Vision Algorithm for the on-board SBSS is implemented. It receives the input data from the IPF-Manager. Input data are configuration parameters and images received as a streaming of pixels to increase the performance of the system. The internal hardware implementation of the image processing includes a combination of the algorithms described. The initial stages of both algorithms are common and therefore the resources are shared for an efficient implementation.

The main submodules for common stage within the IP-Core are:
- Cropping
- Binarisation
- Masking

All of these common functions are implemented as a cascade of stages in a pipelined streaming design. After the common stages, the streaming is divided in two different paths executed in parallel. Once the execution is completed the module will provide a unified output with the features of the Debris detection if exist. The output is sent to IPF Manager through a Telemetry.

The main submodules within the IP-Core Path 1 are:
- Candidates Detection-1
- Segmentation
- Center of Brightness Calculation

The main submodules within the IP-Core Path 2 are:
- Morphological operations (Dilation, Closing, Erosion, Opening, etc)
- Segmentation
- Candidates Detection-2
- Tracking Stage

Candidates-detection modules of paths 1 and 2 performs different operations and requires a specific implementation for each one. Segmentation modules are implemented using an optimized approach by using a

pipeline with a single pass connected component algorithm by extracting the required blob features.

IPF-Manager module is in charge of the FPGA Control. It includes the Telemetry and Telecommands (TM/TC) functionality which is in charge of decoding/encoding all the messages interchanged with CIF. The VDDT HW IP core will receive commands and send result and status through the IPF Management & TM/TC block in accordance to the designed interface. The systems includes a DDR II memory directly connected to IPF. This module acts as a memory controller to effectively manage the access for write/read operations required by VDDT-HW-IP for storing intermediate data while Image Processing Execution.

The IPF module implements the interface between the IPB-CIF (Master) and the IPB-IPF (Slave). The communication is parallel and bidirectional in order to facilitate the transfer of information.

In addition to the rest of the FPGA logic, a Housekeeping block is periodically monitoring the FPGA health status and performance by reading the on-chip temperature measurement and power supply. It generates and send a periodic TM message including health status

8. IP HARDWARE TESTS

8.1. Data Generation for tests
All the data needed to execute the tests has to be collected and processed in order to generate the inputs of tests. Synthetic images are generated considering the data coming from the analysis run with the PROOF software described in the Observability Analysis (2.3).

To extend the representativeness of the validation tests, two different image generation tools have been used. The first one is the Planet and Asteroid Natural-Scene Generation Utility (PANGU-4) which is a software tool for simulating and visualizing the surface of various planetary bodies including asteroids. It generates a dataset of images based on selected orbital trajectories of Galileo and its attitude used for the validation campaign. Software and HW implementation of IP and PANGU are used to feed the SBSS-GNSS with feature data. *Real world* values of orbital state and attitude state are stored together with measurements data and images, which allow the performance verification of the developed IP. The approach used with this software present multiple advantages:
- It simulates orbital dynamics based on precise numerical calculations.
- It uses CAD model of debris
- It uses a star catalogue, in this case the tycho-2 catalogue.

However, while developing the use cases it was detected that magnitudes are sometimes not

photorealistic. This distortions tend to appear for objects represented in the camera frame below 1 pixel of resolution.

To mitigate the aforementioned disadvantage, a complementary second image generation tool has been developed. It is a Matlab script that includes several user defined parameters to control its behavior such as star rate, star distribution and movement direction, target magnitude, RMS of the target rate and much more. It isn't based on a real star catalogue, instead, the images are generated randomly with the set characteristics. The main advantages are:

- It is possible to select a desired star density.
- It offers more flexibility and variability when changing parameters, due to the in-depth knowledge.

Considering all factors involved in these generation methods, the conclusion is that both can be used complementary. Where PANGU can be used as a true simulation of the behavior of the camera frame on-board for selected orbital trajectories. The Matlab script can be used to generate more test cases that will be unlikely to be encountered, but improves the robustness of the tests.

8.2. Model in the Loop Tests (MIL)

A software version is used as a model of the Image Processing Algorithm described. It is performed before IP-Hardware validation to assess the functional behavior of the model. During the execution of the IP MIL tests, the images and the trajectory data are generated and collected in order to be used in the following tests.

The test cases proposed in section 8.4 are common for MIL and FIL, therefore, intermediate and final results can be compared.

8.3. Unitary and Integration Tests

All the internal modules and sub-blocks of each subsystem of the image processing, unit management modules, interfaces and other FPGA related functionalities are individually validated after implementation by comparing the HW implementation against the equivalent output of the existing SW implementation using FPGA Simulation tools (behavioral, synthesis and post place & route simulations). Incremental integration tests are performed until the whole system is validated.

8.4. FPGA in the Loop (FIL) – Test Cases

To limit the number of executed tests without affecting the test representativeness, three main objectives are defined:

- Debris apparent magnitude influence
- Dwell rate and debris orbit influence
- Exposure time influence

FIL-Test	Objective	Apparent Magnitude	Dwell Rate (Range)	Exposure	Tool
# 1	Debris apparent magnitude influence	9	1 pxl/s	4s	Matlab
# 2		11	1 pxl/s	4s	Matlab
# 3		13	1 pxl/s	4s	Matlab
# 4	Dwell rate and debris orbit influence	11	0.5 pxl/s	4s	Matlab
# 5		11	2 pxl/s	4s	Matlab
# 6		11	4 pxl/s	4s	Matlab
# 7	Exposure time influence	11	1 pxl/s	2s	Matlab
# 8		11	1 pxl/s	6s	Matlab
# 9		11	1 pxl/s	8s	Matlab
# 10	Realistic Orbital Motion	Dependent on the relative orbital distance, with the following debris parameters: albedo 0.3 1-m diameter	4.1 pxl/s	4s	PANGU
# 11			1.4 pxl/s	4s	PANGU
# 12			1.5 pxl/s	4s	PANGU
# 13			7.5 pxl/s	4s	PANGU

Table 3: Image Processing-HW Test Cases

8.5. FPGA in the Loop (FIL) – Setup and Results

During FPGA in the loop tests, the Image Processing Board (IPB) is connected with an external computer by means of a SpaceWire to USB Brick. This computer supply the test cases orbits input data for the Image Processing System. Thus, the system test execution consists of receiving all the images generated and algorithm execution in the Image Processing Board (IPB). The output of the test execution is the list of tracked debris where each one is represented by a unique identifier and a 2D position vector in the corresponding frame.

After Image Processing Hardware Execution the results obtained are analyzed. The criteria to considerate an accurate detection for this kind of test is strictly related to the orbit determination techniques used to compute the debris orbit. Considering the angular resolution of the sensor of about 11arcsec/pixel (computed assuming a pixel size of 5.5µm and a focal length of 100mm), the limit of successful detection is set to 3pxl, or approximately 30arcsec. This angular error in the debris detection corresponds to an expected orbit determination error of 150m over a distance of 1000km [4].

According the accurate detection criteria, the error is computed as the difference between the real centroid of the debris and the nearest centroid detection of the IP.

The absolute error corresponds to the module of the Euclidean distance.

$$Error_x = X_{Real} - X_{Detected}$$

$$Error_Y = Y_{Real} - Y_{Detected}$$

$$Error_{Mod} = \sqrt{Error_X{}^2 + Error_Y{}^2}$$

After processing the entire trajectory, the following metrics are obtained to evaluate results globally. The average absolute error is calculated as the sum of all the available errors in the whole trajectory. The standard deviation of the absolute error is calculated taking the entire population of the available errors if any.

$$\overline{Error} = \frac{\sum Error_{Mod}}{n\_frames}$$

$$\sigma = \sqrt{\frac{\sum(\overline{Error} - Error_{Mod\_i})^2}{n\_frames}}$$

The algorithm tracking requires an internal latency of three frames due to the internal image integration.

The *Table 4* summarizes the behavior of the system in all test cases.

FIL-Test	AVG ABS	STD DEV
# 1	0,55	0,75
# 2	0,83	0,90
# 3	0,83	0,90
# 4	1,09	0,60
# 5	1,12	1,48
# 6	1,12	1,48
# 7	0,66	0,57
# 8	1,25	1,15
# 9	2,33	4,96
# 10	1,90	2,27
# 11	0,88	0,48
# 12	2,71	2,60
# 13	2,44	1,50

Table 4: Test Cases IP-HW Results

As a graphical visualization of the Image Processing evaluation, the results of Test Case 13 are shown in *Figure 3* and *Figure 4*, where are represented the detection error for each frame, the sum of dataset of 40 input images and the sum of the outputs detected by the IP.
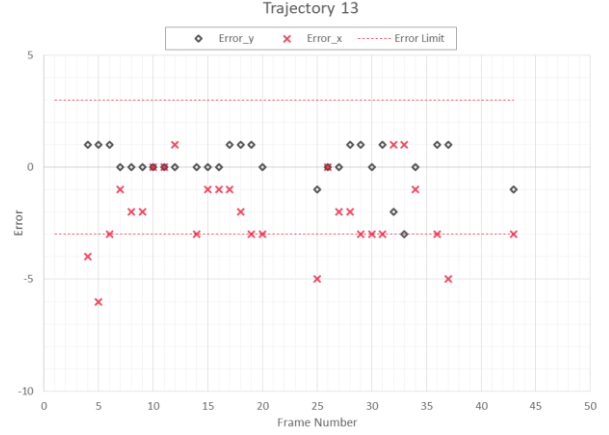

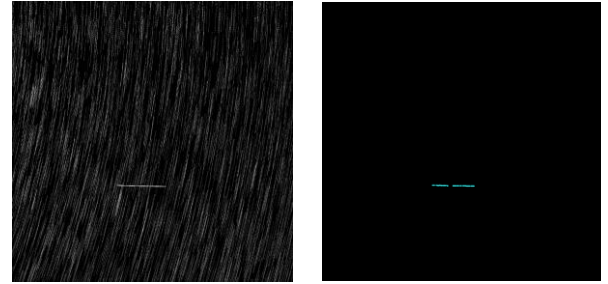*Figure 3: Test Case 13 Debris Detection Error*

Figure 4: Test Case 13. Input images summation of 40 frames (Left). IP Debris Detection Summation (Right)

The results of Image Processing tests confirm the algorithm suitability for debris detection in all cases where the camera sensor is capable to capture the debris in the image. The debris has been successfully detected and in most cases the accurate detection criteria is satisfied, so the error remains below the 3 pixels margin. The average absolute error confirm numerically this fact along the trajectory of all Test Cases, since it is always lower than 3. Standard deviation also remains very low, except in Test Case #9 where the IP output of the centroid in one frame is slightly displaced due to a discontinuity in the integrated image. Along the trajectories some false positives are detected but can be easily discarded after post-processing.

In Test Cases 3 and 6 the IP is not able to detect any debris due to the high apparent magnitude (#3) and high speed (#6). This problem is not related to the underlying detection algorithm, but, given the imposed apparent magnitude, dwell rate of the debris and exposure time, the debris is not visible and, therefore, the camera sensor is not able to capture in the image.

CONCLUSION

This paper present an in-orbit space-based surveillance system experimental payload based on a miniaturized space-qualifiable concept using high-performance computer-vision algorithms solution and its implementation deployed in a dedicated HW avionics specifically designed in the frame of this work in the ESA-H2020 project named SBSS-GNSS. Space-based assets can be used to complement and enhance the capabilities of a ground-based network of sensors (mainly surveillance and tracking radars and optical telescopes. The proposed experimental payload consists on a miniaturized independent system, conceived as a smart-sensor autonomous payload which is able to detect and track debris through dedicated image processing algorithms accelerated on-board by a HW implementation based on high-performance rad-hard FPGA. The SBSS-GNSS would be eventually hosted as experimental payload on board Galileo satellites of Galileo constellation for offering debris surveillance with main focus in Galileo orbits (MEO) as secondary service for monitoring and detection the proliferations of debris in the most populated space area. Hosting the SBSS-GNSS payload on a Galileo satellite would seem a cost-effective approach besides the technical and operational benefits that will provide thanks to the absence of atmosphere and good timelines, not weather-based degradation and reduction of communication in between ground stations and satellite.

The technical contribution includes avionics solution concept of a reduced volume in cost-effective architecture exploiting high-performance processing needed for the on-board algorithms in the proposed autonomous secondary service eventually to be hosted on Galileo next-generation satellites with the minimum, or none, impact..

These algorithms focus on the detection of faint objects in on-board camera images, identifying light curves and discriminating artificial objects from background stars.

The project starts with concept analysis from mission and environment perspective trading-off different approaches and increase the maturization of the solution up to an elegant prototype manufacturing model of the solution that embeds camera optics, baffle, sensor, FPGA and PCB design.

The project is not yet finalized, facing the final part of the test campaign for HW-in-the-loop validation. This paper presents results for Model-in-the-loop and FPGA-in-the-loop where there were up to 13 different trajectories of relative dynamics of Galileo hosted satellite and emulated debris in the FOV of the camera. The error is computed as the difference between the real centroid of the debris and the nearest centroid detection of the IP. The average absolute error is calculated as the sum of all the available errors in the whole trajectory images. The worst result appears in trajectory 11 with an average absolute error of 2,71 pixels while the average of all trajectories is 1,36 pixels. The results of Image Processing tests confirm the algorithm suitability for debris detection in all cases where the camera sensor is capable to capture the debris in the image. The debris has been successfully detected and in most cases the accurate detection criteria is satisfied, so the error remains below the 3 pixels margin.

REFERENCES

[1] Gonzalez Arjona D., Bajanaru P., Domingo R., Stancu F.A., Alexe A.L., Gogu D.G., Sincan S. "On-Board Complex Image Processing Based On FPGA Acceleration For Autonomous Navigation In Space" On-Board Data Processing Conference, European Space Research and Technology Centre, European Space Agency, 2019

[2] Kasunic, Keith J. Optical systems engineering. McGraw-Hill Education, 2011.

[3] Krag, H., et al. "PROOF—The extension of esa's MASTER Model to predict debris detections." Acta Astronautica 47.2-9 (2000): 687-697.

[4] Kim, Simon, et al. "Analysis of space debris orbit prediction using angle and laser ranging data from two tracking sites under limited observation environment." Sensors. 20(7), 1950 (2020)